Estimation of Multiple Specific Growth Rates in Bioprocesses

An on-line estimation technique for multiple specific growth rates is proposed. Time-varying tuning parameters are used to obtain constant estimation error dynamics in spite of strongly varying process dynamics commonly encountered in bioprocesses. This approach simplifies the tuning of the algorithm to a pole placement procedure. Application of the method is illustrated through the study of the baker's yeast fed-batch process. Guidelines for selection of measured state variables are given in relation to the performance of the estimation method.

Yves Pomerleau
Michel Perrier
Biotechnology Research Institute
6100 Royalmount Avenue
Montréal, Canada H4P 2R2

Introduction

In biotechnological processes, the use of the specific growth rate to describe the reaction rate is a simplication of a complex set of more than 1,000 biochemical reactions combined with physical transfer rates. The task of obtaining an analytical expression relating the specific growth rate to the extra-cellular physico-chemical variables in a wide range of conditions is a difficult one, especially in the case where the organism may use more than one catabolic pathway. The determination of the parameter values for these analytical expressions also suffers from identifiability problems (Holmberg, 1982). These difficulties have conducted many researchers working in bioreactor control to avoid such analytical expressions and to consider the specific growth rate as a time-varying parameter of a nonstationary system to be estimated on-line (Nihtila et al., 1984; Stephanopoulos and San, 1984; Dochain, 1986).

In this paper, the method proposed by Dochain and Bastin (1985) is improved by a time-varying tuning parameter procedure which increases the performance of the method and makes it more robust in the case of time-varying process dynamics. This method is preferred to an optimal one, like the Extended Kalman filter, because of the advantage that its stability and convergence can be demonstrated. Also, it avoids the problem of linearizing the model for processes not having any fixed operating point (e.g., batch and fed-batch processes).

The case study presented here is the baker's yeast fed-batch process with multiple specific growth rates to be estimated in a strongly nonlinear and time-varying dynamics environment. The yeast may use three catabolic pathways in this process: sugar oxidation, sugar fermentation with ethanol as an end product, and ethanol oxidation when the conditions are favorable. The distribution of substrate fluxes through these three catabolic pathways depends on the process conditions and is well known as the Crabtree and Pasteur effects. Recently, many workers associated a specific growth rate with each of these catabolic pathways instead of using a global one (Sonnleitner and Kappeli, 1986; Engasser, 1985; Liviense, 1984). This approach is used in the present work, and each of the three specific growth rates are estimated on-line; this allows a better insight of the process conditions.

The process model including the three specific growth rates is presented in the next section. It is followed by the description of the design of the specific growth rates estimator for the time-continuous case. A discrete version is also described and used in this work. The time-varying procedure for the selection of tuning parameters follows. An evaluation of the performance of the estimator is presented using simulation data. Finally, guidelines are given for the selection of measured state variables.

Process Model

The process model for baker's yeast production in fed-batch is obtained from a mass balance on biomass, substrate, ethanol, dissolved oxygen, and carbon dioxide. In the mass balance, the global specific growth rate and the global yield are divided in three parts associated with each catabolism. The equations, in terms of concentration, are written as follows:

$$\begin{aligned}
dx/dt &= (\mu_o + \mu_r + \mu_e - D) * x \\
ds/dt &= D * (s_i - s) \\
&\quad + (-\mu_o/Y_o - \mu_r/Y_r) * x \\
de/dt &= -D * e + (\mu_r/Y_{re} - \mu_e/Y_e) * x \\
dc/dt &= -D * c + OTR \\
&\quad + (-\mu_o/Y_{o2} - \mu_e/Y_{o2e}) * x \\
dg/dt &= -D * g + CTR \\
&\quad + (\mu_o/Y_{go} + \mu_r/Y_{gr} + \mu_e/Y_{ge}) * x \\
dV/dt &= D * V = F.
\end{aligned} \tag{1}$$

Correspondence concerning this paper should be addressed to M. Perrier.
Y. Pomerleau is presently with the Ecole Polytechnique de Montréal.

Table 1. Yield Coefficient Values

Coefficients	Values	
Y_o	0.49	g biomass/g sugar
Y_r	0.05	g biomass/g sugar
Y_{re}	0.10	g biomass/g ethanol
Y_e	0.72	g biomass/g ethanol
Y_{o2}	1.20	g biomass/g oxygen
Y_{o2e}	0.64	g biomass/g oxygen
Y_{go}	0.81	g biomass/g CO_2
Y_{gr}	0.11	g biomass/g CO_2
Y_{ge}	1.11	g biomass/g CO_2

In this mass balance, the gas-phase dynamics is neglected, the reactor is assumed to be perfectly mixed, ethanol evaporation is neglected, and the yield coefficients are assumed to be known and constant. Table 1 presents the values used for the yield coefficients.

When using only a global specific growth rate for this process, the yield coefficients vary strongly. Using three specific growth rates allows one to obtain nearly constant yield coefficients. Without the constant yield coefficient assumption, observability problems could be encountered.

The process model can be formulated in the following state space representation (Dochain et al., 1988):

$$d\xi/dt = -D * \xi + K * \varphi * x + U \tag{2}$$

where

ξ = state variables vector $[x\ s\ e\ c\ g]^T$, dimension N

φ = specific growth rates vector $[\mu_o\ \mu_r\ \mu_e]^T$, dimension M

U = input/output vector $[0D * s_i\ 0\ \text{OTR}\ \text{CTR}]^T$, dimension N

K = yield coefficients matrix, dimension $N \times M$

$$= \begin{bmatrix} 1 & 1 & 1 \\ -1/Y_o & -1/Y_r & 0 \\ 0 & 1/Y_{re} & -1/Y_r \\ -1/Y_{o2} & 0 & -1/Y_{o2e} \\ 1/Y_{go} & 1/Y_{gr} & 1/Y_{ge} \end{bmatrix}$$

This matrix representation of the model is applicable to a wide range of batch, continuous and fed-batch biotechnological processes with a single organism and, with minor modifications, to processes involving more than one organism.

Analytical expressions for the specific growth rates are introduced in this model only for simulation purposes. The analytical expressions of Sonnleitner and Kappeli (1986) and their parameter values are used, except for the maximum oxygen uptake rate which is chosen to reduce the critical specific growth rate to a value of 0.2 h^{-1}. The choice of the growth kinetics model has no impact *per se* on the estimator design and performance.

Nonlinear Estimation of the Specific Growth Rates

The state space representation (Eq. 2) can be divided in two partitions: the first partition includes the equations relative to the measured state variables; the second partition, the equations relative to the nonmeasured state variables. For the present development, we consider that the measured state variables are the ethanol, dissolved oxygen and carbon dioxide concentrations in the broth. The state space model can now be expressed as:

$$d\xi_1/dt = -D * \xi_1 + K_1 * \varphi * x + U_1 \tag{3}$$

$$d\xi_2/dt = -D * \xi_2 + K_2 * \varphi * x + U_2 \tag{4}$$

where

$\xi_1 = [e\ c\ g]$, measured state variables vector

$\xi_2 = [x\ s]$, nonmeasured state variables vector

K_1, K_2, U_1, U_2 = division of K and U according to each partition

The elements of the input/output vector U_1, in this case OTR and CTR, need also to be measured.

Biomass concentration observer

The design of the specific growth rates estimator uses the measured state variables partition. The estimator, however, requires a biomass concentration observer since the unknown biomass concentration appears in the equation of this partition (Eq. 3). The approach chosen follows the work of Dochain et al. (1988). A transformation is applied to the nonmeasured state variables partition:

$$Z = \xi_2 - K_2 * K_1^{-1} * \xi_1 \tag{5}$$

and the following new nonmeasured state variables partition is obtained:

$$dZ/dt = -D * Z + U_2 - K_2 * K_1^{-1} * U_1 \tag{6}$$

The new state space model formed by Eqs. 3 and 6 is equivalent to the original state space model. In this approach, the number of state variables to be measured has to be at least equal to the number of specific growth rates to be estimated in such a way that the inverse or pseudoinverse of the matrix K_1 exists.

The asymptotic state observer is obtained from the new nonmeasured state variables partition:

$$d\hat{Z}/dt = -D * \hat{Z} + U_2 - K_2 * K_1^{-1} * U_1$$
$$\hat{\xi}_2 = \hat{Z} + K_2 * K_1^{-1} * \xi_1 \tag{7}$$

With a good initial estimate of Z, the trajectories of $\hat{Z}$ and of the nonmeasured state variables can be evaluated when the measured values of ξ_1, U_1 and U_2 become available. The asymptotic convergence of this observer has been proved by Dochain et al. (1988). An evaluation of the performance of this observer as applied to the biomass concentration is presented in following sections.

Estimator design

The first step in the specific growth rates estimator design is to perform a transformation on the measured state variables partition in order to decouple the equations with respect to the specific growth rates. The following transformation is applied:

$$\Psi = K_1^{-1} * \xi_1 \tag{8}$$

The new measured state variables partition is then:

$$d\Psi/dt = -D * \Psi + \varphi * x + K_1^{-1} * U_1 \tag{9}$$

From this system, the specific growth rates estimator is:

$$\begin{aligned} d\hat{\Psi}/dt &= -D * \Psi + \hat{\varphi} * \hat{x} + K_1^{-1} * U_1 \\ &\quad + C_1 * (\Psi - \hat{\Psi}) * \hat{x} \\ d\hat{\varphi}/dt &= C_2 * (\Psi - \hat{\Psi}) * \hat{x} \end{aligned} \tag{10}$$

where C_1 and C_2 are diagonal matrices containing design parameters. The form of this nonlinear estimator is typical: estimates of the transformed measured state variables ($\hat{\Psi}$) are produced with the process model incorporating the specific growth rates estimates ($\hat{\varphi}$), and these estimates are in turn corrected according to the errors between the transformed measured state variables and their estimates. The presence of the measured state variables (Ψ) in the first term of the righthand side instead of the estimate values ($\hat{\Psi}$) is a particular case of the estimator model presented by Narenda and Annaswamy (1989). The expressions chosen for the filter gains, $C_1 * \hat{x}$ and $C_2 * \hat{x}$, are much simpler than those of the corresponding Extended Kalman filter. Dochain (1986) has rigorously proved the stability and convergence of the single variable version of this algorithm in many examples of bioprocesses.

Tuning of the Algorithms

For the continuous version of this algorithm, Dochain (1986) proved that the algorithm is stable and converges when all the elements of C_1 and C_2 are positive. For the discrete version, obtained by Euler approximation, this condition is no longer sufficient. The values of C_1 and C_2 have to be chosen more carefully. For the choice of these tuning parameters, we can use the estimation error system obtained from the difference between the process equation and the estimator algorithm. Since the estimator for the three specific growth rates is completely decoupled, we examine only the behavior of the oxidative specific growth rate estimation which also applies to the two others.

The equations describing the estimation error dynamics of the oxidative specific growth rate, assuming that the observed biomass concentration is equal to the real one, can be written as follows:

$$\begin{bmatrix} \tilde{\Psi}_{1t+1} \\ \tilde{\mu}_{ot+1} \end{bmatrix} = \begin{bmatrix} 1 - c_1 * T * x & T * x \\ -c_2 * T * x & 1 \end{bmatrix} * \begin{bmatrix} \tilde{\Psi}_{1t} \\ \tilde{\mu}_{ot} \end{bmatrix} + \begin{bmatrix} 0 \\ 1 \end{bmatrix} * (\mu_{ot+1} - \mu_{ot}) \tag{11}$$

where

$$\tilde{\Psi}_1 = \Psi_1 - \hat{\Psi}_1$$

$$\tilde{\mu}_o = \mu_o - \hat{\mu}_o$$

T = sampling interval

The poles of this system are:

$$p_1, p_2 = 1 - c_1 * T * x/2 \pm T * x/2 * \sqrt{c_1^2 - 4 * c_2} \tag{12}$$

For constant values of c_1 and c_2, the speed of convergence increases as the biomass increases because this system is nonstationary due to the presence of the biomass concentration (x) in Eq. 12. It then follows that tuning has to be done according to the highest expected level of biomass concentration. In the fed-batch process, the maximum biomass concentration is reached at the end of the fermentation and is typically 4 to 6 times the initial concentration. This method of tuning will cause an unnecessary slow convergence of the estimation algorithm at the beginning of the fermentation as it can be seen in Figure 1.

This undesirable effect can be avoided by using time-varying design parameters. These parameters can be chosen to obtain a constant speed of convergence during all the process: the values of c_1 and c_2 become a function of the biomass concentration. The trajectories of c_1 and c_2 can be selected to obtain constant pole positions of the estimation error dynamics in spite of the nonstationary nature of the system. Our choice is to fix a double pole by relating c_2 as a function of c_1. Then, c_1 is selected to position this double pole according to the desired dynamics. The trajectories of c_1 and c_2 that fulfill these requirements are:

$$\begin{aligned} c_2 &= c_1^2/4 \\ c_1 &= 2 * (1 - p)/T/x \end{aligned} \tag{13}$$

where p is a pole position in the Z-plane.

Because the expressions for c_1 and c_2 are only function of the biomass concentration, the same trajectories are obtained for the estimators of the fermentative specific growth rate and of the oxidative growth rate on ethanol. Instead of having six parameters to adjust, two for each metabolism, the tuning of the three specific growth rates estimator is done with a single coefficient (p) with a physical significance: a pole in the Z-plane. The

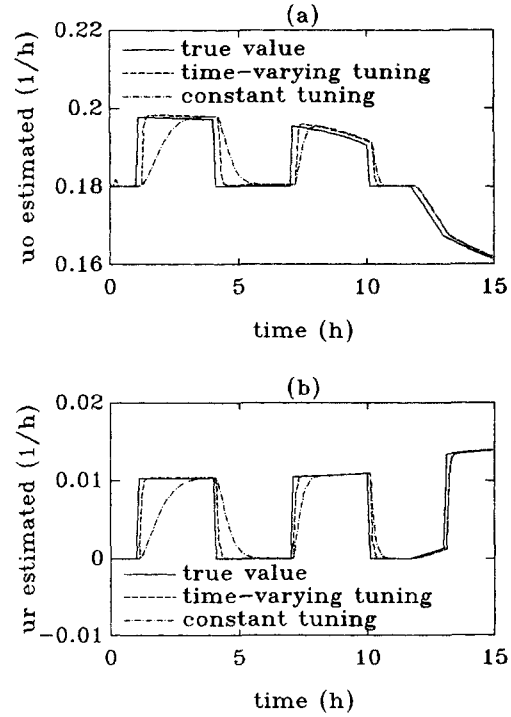

Figure 1. Influence of the tuning method on the speed of convergence.

general estimator algorithm in its discrete version can be written as:

$$\hat{\Psi}_{t+1} = \hat{\Psi}_t + T * [-D_t * \Psi_t + \hat{\varphi}_t * \hat{x}_t + K_1^{-1} * U_{1t} + 2/T * (1 - p)(\Psi_t - \hat{\Psi}_t)]$$
$$\hat{\varphi}_{t+1} = \hat{\varphi}_t + (1 - p)^2 * (\Psi_t - \hat{\Psi}_t)/\hat{x}_t/T \qquad (14)$$

Results and Discussion

In the evaluation of the estimator performance, two sets of data resulting from simulation runs are used. In both cases, data were obtained by adjusting the substrate feed rate to impose a pulsed profile of the substrate concentration in the broth in order to test the algorithm under the different dynamics of the process. As a result, the specific growth rates also follow a pulsed profile until the oxygen transfer rate becomes a limiting factor. In the first set of data, the further oxidation of ethanol by yeast was eliminated from the model ($\mu_e = 0$). These data are used to investigate the estimator performance when only two state variables are measured and two specific growth rates are to be estimated (μ_o, μ_r). The second data set was produced using the complete model, including the ethanol consumption. The performance of the three specific growth rates estimator for the second data set is evaluated based on three measured state variables. The performance of the estimator design omitting the ethanol consumption metabolism is also evaluated in the case of the complete simulation model.

All the results presented in this paper are obtained with the discrete version of the algorithm with a sampling period of 0.1 h. The double-pole position is fixed at 0.1, except otherwise stated. The pole at 0.1 corresponds to a time constant of 0.04 h.

Case 1: simulation without ethanol consumption

Measured State Variables: e and c. When ethanol consumption is neglected, only two state variables have to be measured. Among the possible combinations of two measured state variables, that of ethanol with dissolved oxygen is attractive since it is the only combination for which the equations in the measured state variables partition are already decoupled with respect to the specific growth rates. This allows us to write the algorithm directly in terms of the state variables. The discrete version, obtained by Euler discretization, with time-varying expressions for c_1 and c_2 defined by Eq. 13 is then for the oxidative specific growth rate:

$$\hat{c}_{t+1} = \hat{c}_t + T * [-D_t * c_t - \hat{\mu}_{ot} * \hat{x}_t/Y_{o2} + OTR_t + 2/T * (1 - p) * (c_t - \hat{c}_t)]$$
$$\hat{\mu}_{ot+1} = \hat{\mu}_{ot} - (1 - p)^2 * (c_t - \hat{c}_t) * Y_{o2}/\hat{x}_t/T \qquad (21)$$

whereas the fermentative specific growth rate estimator gives:

$$\hat{e}_{t+1} = \hat{e}_t + T * [-D_t * e_t + \hat{\mu}_{rt} * \hat{x}_t/Y_{re} + 2/T * (1 - p) * (e_t - \hat{e}_t)]$$
$$\hat{\mu}_{rt+1} = \hat{\mu}_{rt} + (1 - p)^2 * (e_t - \hat{e}_t) * Y_{re}/\hat{x}_t/T \qquad (22)$$

As pointed out earlier, the tuning value of parameter p is the same in Eqs. 21 and 22.

Figure 1 presents the results of the estimation procedure obtained with constant tuning parameters adjusted to the final biomass concentration and with time-varying tuning algorithm based on a fixed value of the pole p. For constant tuning parameters, the speed of convergence is very slow at the beginning of the fermentation. An increase of the speed by changing the tuning parameters may produce oscillatory patterns at the end of the fermentation and even unstable estimates (results not shown). With time-varying tuning parameters, the speed of convergence is constant throughout the course of the process and follows the desired dynamics. No difference of performance was noticed between the nonlimited and limited oxygen transfer rate regions of the process in spite of different dynamic regimes.

The performance of the biomass concentration observer is shown in Figure 2. In graph a, the error percentage on biomass concentration is shown with and without noise on the measurement: relative error with uniform distribution of ±5% and ±10% were added to ethanol and dissolved oxygen concentrations as well as to oxygen transfer rate. The observation error on biomass concentration remains within ±0.5% in the ±5% case and within ±1% in the ±10% case. In graph b, the evolution of the observation error with an initial error of ±10% on the biomass concentration is illustrated. In spite of the important initial error, the biomass concentration observer still converges with dynamics imposed by the dilution rate.

The response of the specific growth rate estimator using wrong initial estimates of $\hat{\mu}_o$ and $\hat{\mu}_r$ and of the state variables is shown in Figure 3. The parameter estimates converge quickly. The performance is not as good in the case of a wrong initial estimate of the biomass concentration as shown in Figure 4. The estimation error is higher in this case, but $\hat{\mu}_o$ and $\hat{\mu}_r$ still converge on their real values at a speed corresponding to the biomass con-

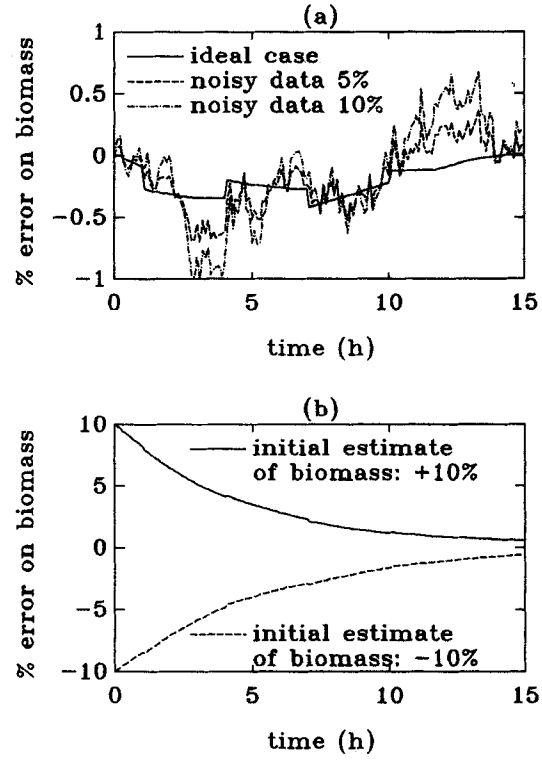

Figure 2. Influence of noise and wrong initial estimate of biomass concentration on the observer performance.

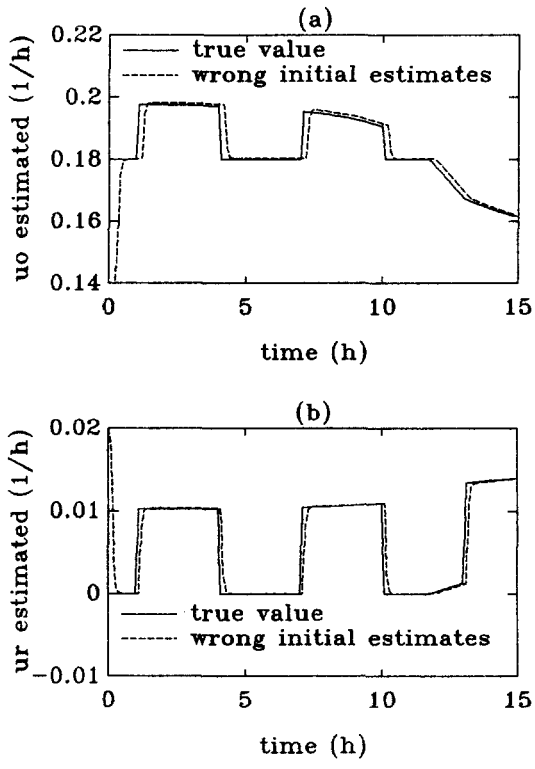

Figure 3. Influence of wrong initial values of estimates on the estimator performance.

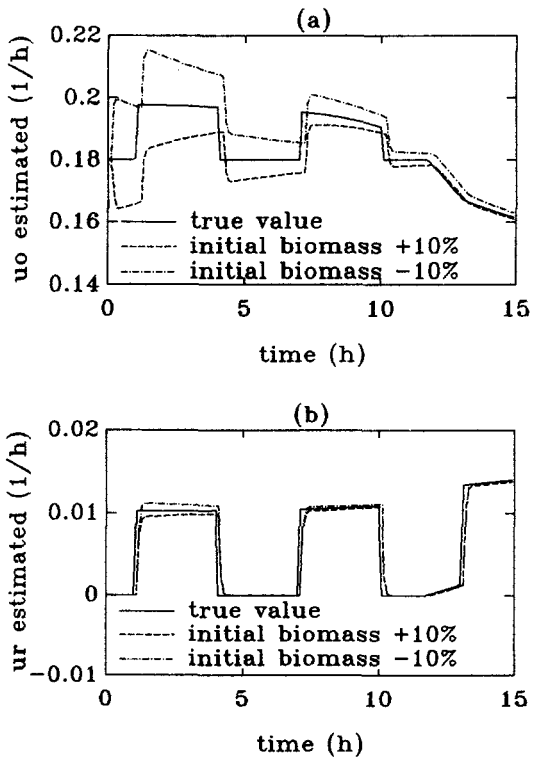

Figure 4. Influence of wrong initial estimate of biomass concentration on the estimator performance.

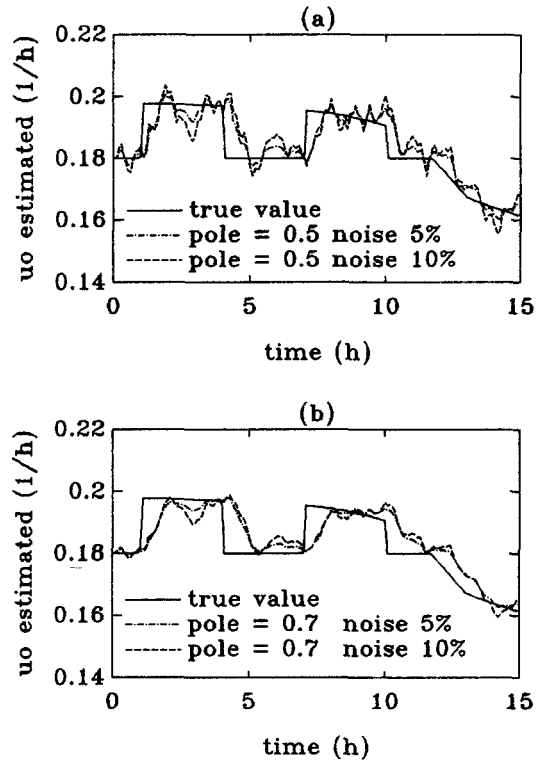

Figure 5. Noise rejection ability of the estimation algorithm.

centration observer dynamics. The oxidative specific growth rate estimator is more sensitive than the fermentative estimator to a wrong initial value of biomass.

The robustness of the algorithm in the presence of noisy data depends on the choice of the desired estimation error dynamics. Figure 5 shows the estimation results in the same cases of noisy data described earlier. Graph a presents the results with the double pole fixed at 0.5 and graph b with the double pole at 0.7. Corresponding time constants are 0.14 h and 0.28 h, respectively. As expected, the desired convergence rate has to be reduced to improve the filtering ability of the estimator.

Comparison with Different Sets of Measured State Variables. The design of biomass concentration observers and specific growth rates estimator for other sets of measured state vari-

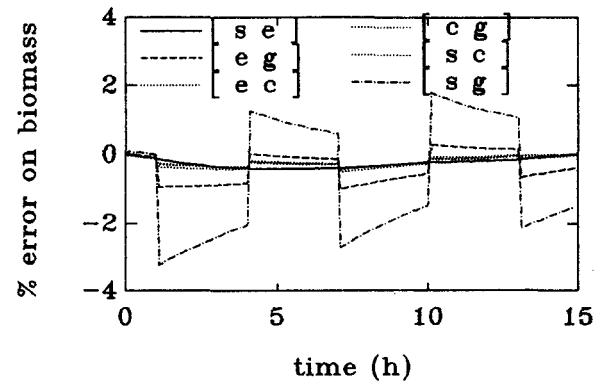

Figure 6. Observer performance using different combinations of two measured state variables.

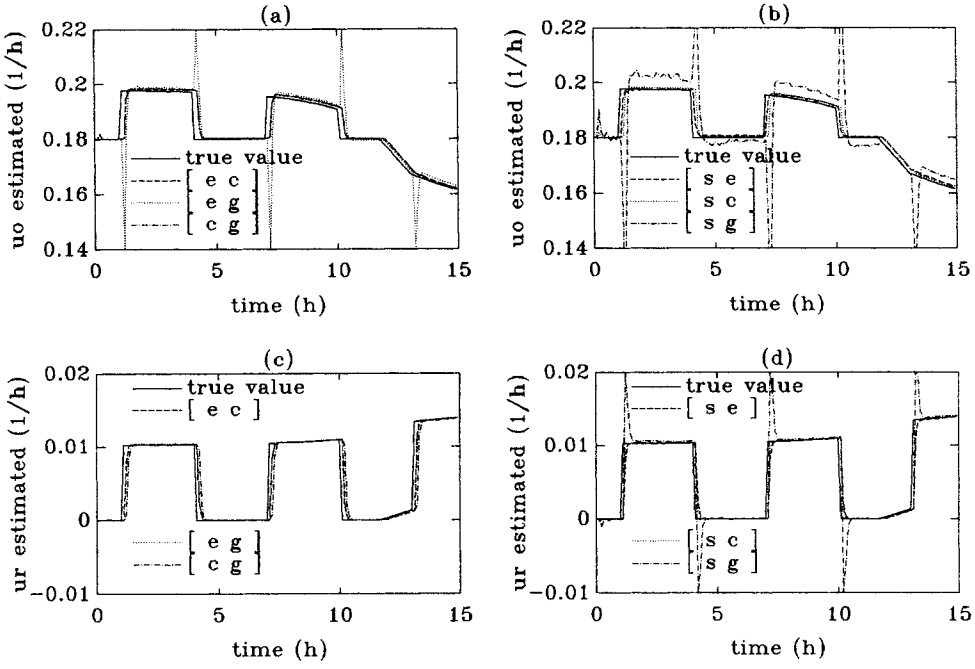

Figure 7. Estimator performance using different combinations of two measured state variables.

ables was also carried out. These sets are:

- Substrate and ethanol [*s e*]
- Substrate and dissolved oxygen [*s c*]
- Substrate and carbon dioxide [*s g*]
- Ethanol and dissolved oxygen [*e c*]
- Ethanol and carbon dioxide [*e g*]
- Dissolved oxygen and carbon dioxide [*c g*]

The response of the biomass concentration observer for all these cases is shown in Figure 6. In four cases, the observation error remains within ±0.5% and within ±1% in the [*e g*] case. In the [*s g*] case, the observer performs badly. This behavior is linked to the fact that the condition number of the yield coefficient matrix of the measured state variables partition is high (Table 2) and that identifiability problems are expected.

Figure 7 shows that the specific growth rate estimates are very sensitive to shifts in the operating conditions for the [*s g*] set of measured state variables. Relating these results to the condition number of matrix K_1 for each combination of measured state variables shown in Table 2, it is seen that the best performance is obtained when the condition number is low.

Case 2: simulation with ethanol consumption

A third specific growth rate has to be estimated when the ethanol consumption cannot be neglected. Three state variables have to be measured to identify the three specific growth rates. Observers for the biomass concentration and estimators for the specific growth rates were designed and evaluated for the following sets of measured state variables:

- Substrate, ethanol and dissolved oxygen [*s e c*]
- Substrate, ethanol and carbon dioxide [*s e g*]
- Substrate, dissolved oxygen and carbon dioxide [*s c g*]
- Ethanol, dissolved oxygen and carbon dioxide [*e c g*]
- Biomass, ethanol and dissolved oxygen [*x e c*]
- Biomass, ethanol and carbon dioxide [*x e g*]
- Biomass, dissolved oxygen and carbon dioxide [*x c g*]

Figure 8 illustrates the response of the biomass concentration observer for cases when biomass concentration is not measured. The observer corresponding to measurement of ethanol, dissolved oxygen and carbon dioxide concentrations performs badly. This may be attributed to the high condition number of the yield coefficients matrix K_1 as shown in Table 3. In other cases, an error of no more than 2% is obtained.

The results for the three specific growth rates estimation

Table 2. Condition Number of Yield Coefficient Matrix for Sets of Two Measured State Variables

Measured Variables Set	Condition Number
[*s e*]	25.
[*s c*]	24.
[*s g*]	85.
[*e c*]	12.
[*e g*]	15.
[*c g*]	11.

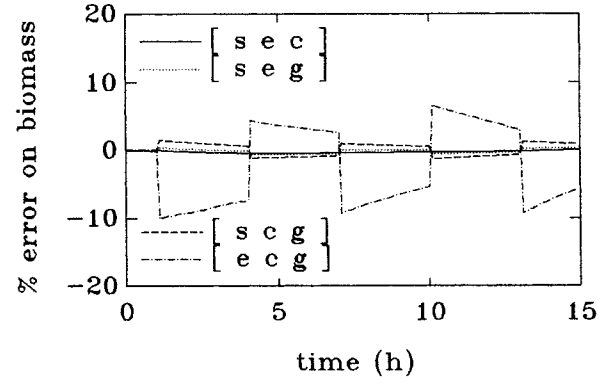

Figure 8. Observer performance using different combinations of three measured state variables.

Table 3. Condition Number of Yield Coefficient Matrix for Sets of Three Measured State Variables

Measured Variables Set	Condition Number
[x e c]	38.
[x e g]	52.
[x c g]	34.
[s e c]	157.
[s e g]	114.
[s c g]	157.
[e c g]	944.

algorithms are shown in Figure 9, 10 and 11 for six sets of measured state variables. The results for the [e g c] case are not shown because of the problem of ill-conditioned matrix K_1 mentioned above. The results for the estimation of oxidative specific growth rate and of the oxidative specific growth rate on ethanol present noisy profiles because the condition number of the yield coefficient matrix is much higher than in the case of two measured state variables. However, the fermentative specific growth rate estimate does not show this behavior.

Figure 12 and 13 show the response of design omitting the ethanol consumption terms in situations where ethanol consumption still occurs. The designs with two and three measured state variables produce no significant difference in the observed biomass concentration (Figure 12). The oxidative specific growth rate estimate using the two measured state variables estimator design shows a bias only when ethanol is consumed (Figure 13). Otherwise, this estimate shows good agreement with the real value. The estimation of the fermentative specific

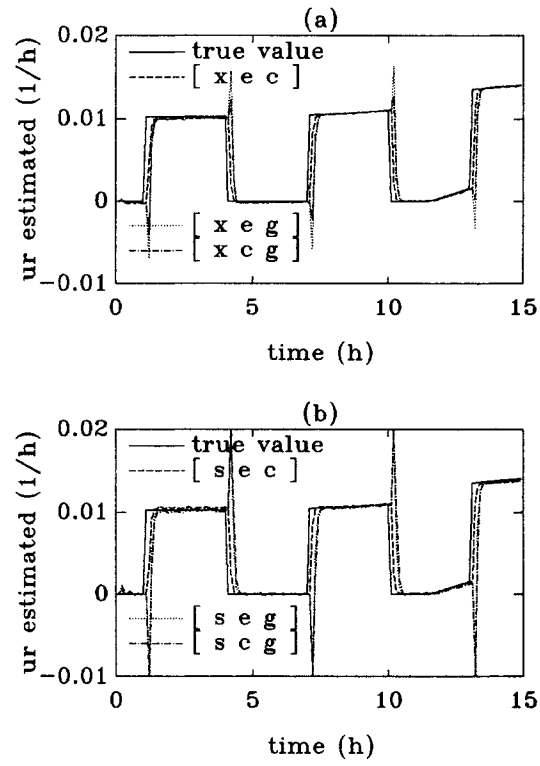

Figure 10. Estimation of fermentative specific growth rate using different combinations of three measured state variables.

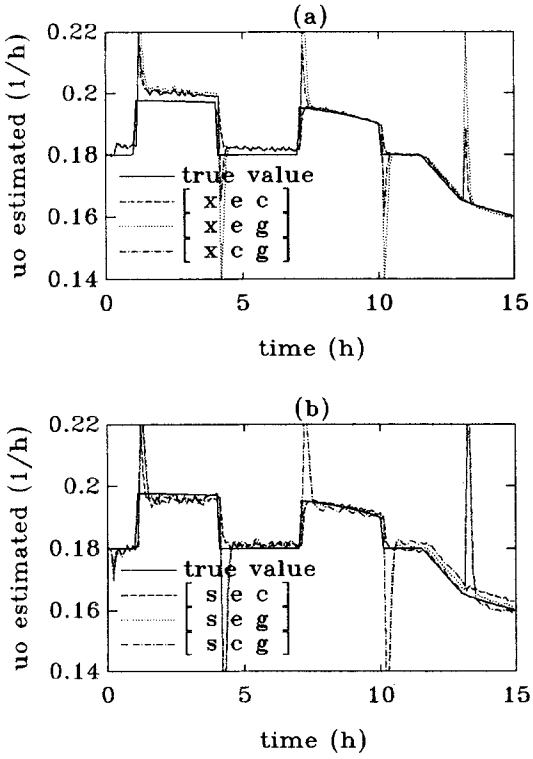

Figure 9. Estimation of oxidative specific growth rate using different combinations of three measured state variables.

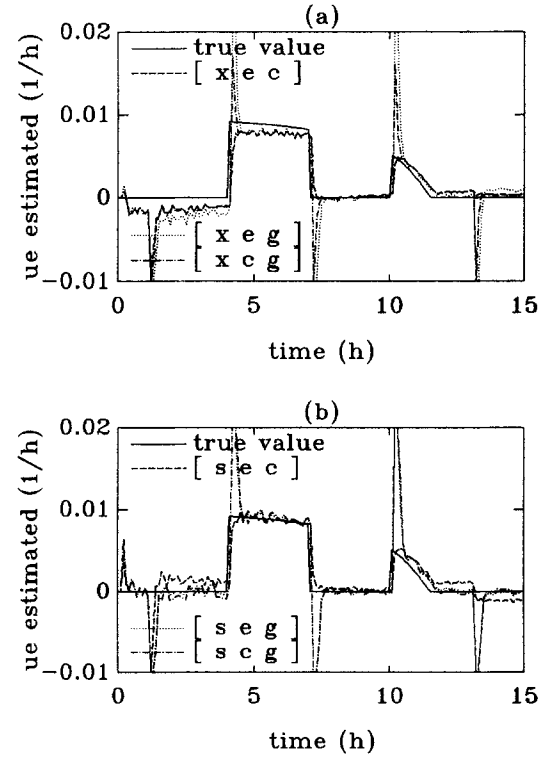

Figure 11. Estimation of oxidative specific growth rate on ethanol using different combinations of three measured state variables.

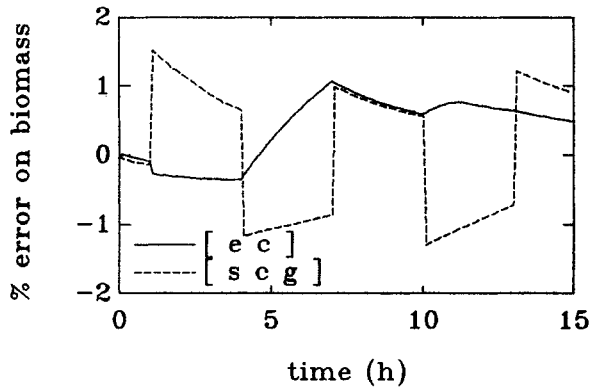

Figure 12. Sensitivity of biomass concentration observer using two or three measured state variables.

growth rate is less affected: the error during the ethanol consumption periods is small.

In Figure 14, the comparison between the two or three measured state variables algorithms is shown in the case of simulation with a typical industrial substrate feeding profile. Ethanol production increases because of the limited oxygen transfer rate ($t > 6$ h), but ethanol is eventually consumed later because of the reduction in the dilution rate ($t > 8$ h). The error on the observed biomass concentration and on the estimates of oxidative and fermentative specific growth rates becomes significant only at the ethanol consumption stage ($t > 12.5$ h) when it is less crucial for the overall productivity of the process.

Conclusion

In this paper, a simple method was presented to design a biomass concentration observer and an estimator for multiple specific growth rates. The method was applied to the baker's yeast fed-batch process where the global specific rate is subdivided in three components in order to reflect the three main catabolisms of the yeast. A new approach using time-varying design parameters was introduced that simplifies the tuning procedure. Instead of having six coefficients to adjust for three estimators, only one parameter is needed and this parameter reflects the desired estimation error dynamics. The tuning procedure also has the advantage to produce constant estimation error dynamics in spite of the nonstationarity of the process.

The method was evaluated by simulation under different conditions and different sets of measured state variables. This investigation showed the good performance of the method except in the case where the condition number of the yield coefficients matrix of the measured state variables partition has high values. If the user has the choice of different sets of measured state variables, the set with the lowest condition number of yield coefficient matrix K_1 should be chosen to obtain the best performance. It was shown also that, for baker's yeast, the estimation algorithm based only on two measured state variables can be used even when ethanol consumption occurs.

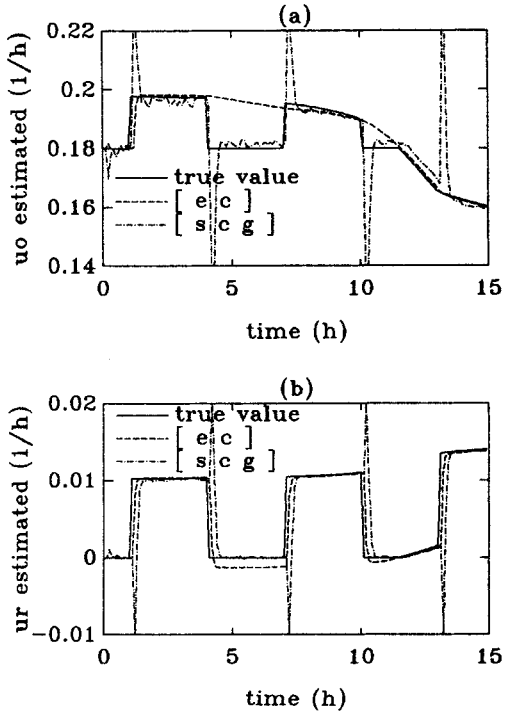

Figure 13. Estimation of μ_o and μ_r with and without neglecting ethanol consumption.

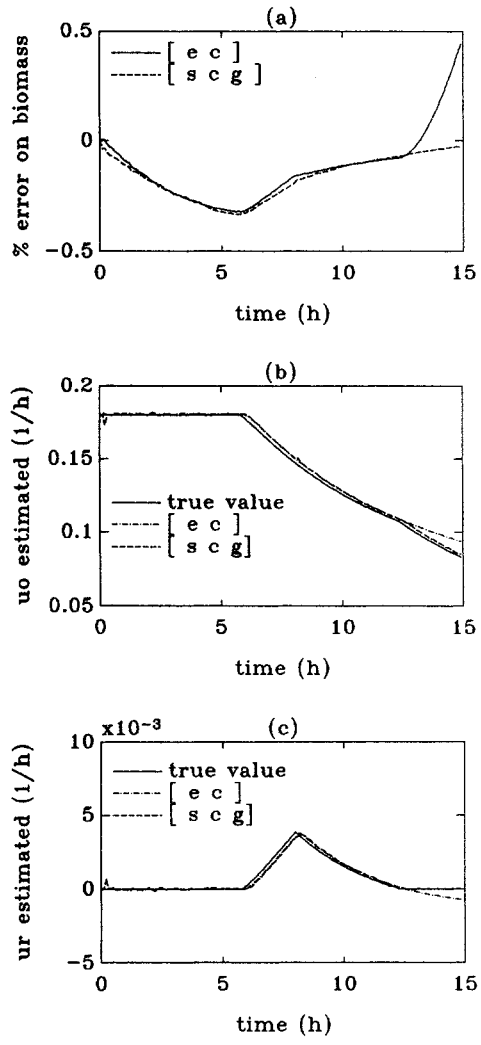

Figure 14. Estimation of biomass concentration and specific growth rates in a typical simulated industrial fermentation.

Acknowledgment

The authors would like to thank Dr. Denis Dochain for stimulating discussions and Dr. Gérald André for useful suggestions and for proofreading the manuscript.

Notation

c = dissolved oxygen concentration
c_1 = diagonal element of design parameters matrix C_1
c_2 = diagonal element of design parameters matrix C_2
C_i = design parameters matrices
CTR = carbon dioxide transfer rate
D = dilution rate
e = ethanol concentration
F = feed rate
g = carbon dioxide concentration
K = yield coefficients matrix
K_i = partition yield coefficients matrices
M = number of specific growth rates
N = number of state variables
OTR = oxygen transfer rate
p = design parameter
p_i = pole in the Z-plane
s = substrate concentration
s_i = substrate concentration in the feed
t = time
T = sampling period
U = input/output vector
U_i = partition input/output vectors
V = volume
x = biomass concentration
Y_e = g biomass/g ethanol by oxidative catabolism on ethanol
Y_{ge} = g biomass/g carbon dioxide by oxidative catabolism on ethanol
Y_{go} = g biomass/g carbon dioxide by oxidative catabolism
Y_{gr} = g biomass/g carbon dioxide by fermentative catabolism
Y_o = g biomass/g substrate by oxidative catabolism
Y_{o2} = g biomass/g oxygen by oxidative catabolism
Y_{o2e} = g biomass/g oxygen by oxidative catabolism on ethanol
Y_r = g biomass/g substrate by fermentative catabolism
Y_{re} = g biomass/g ethanol by fermentative catabolism
Z = transformed state variables vector

Greek letters

ξ = state variables vector
ξ_i = partition state variables vector
μ_e = oxidative specific growth rate on ethanol
μ_o = oxidative specific growth rate
μ_r = fermentative specific growth rate
φ = specific growth rates vector
Ψ = transformed state variables vector
Ψ_i = element of transformed state variables vector

Superscripts

$\hat{}$ = estimated
$\tilde{}$ = error on

Literature Cited

Dochain, D., and G. Bastin, "Stable Adaptive Algorithms for Estimation and Control of Fermentation Processes," *Modelling and Control of Biotechnological Processes, Proc. IFAC Symp.*, Noordwijkerhout, The Netherlands, 37 (1985).

Dochain, D., "On-Line Parameter Estimation, Adaptive State Estimation and Adaptive Control of Fermentation Processes," Doctoral Diss., Université Catholique de Louvain, Belgium (1986).

Dochain, D., E. De Buyl, and G. Bastin, "Experimental Validation of a Methodology for On-Line State Estimation in Bioreactors," Int. Cong. Computer Applications in Fermentation Technology: Modelling and Control of Biotechnical Processes, University of Cambridge, UK (1988).

Engasser, J.-M., "Modélisation physiologique des procédés de fermentation," *Bio-Sci.*, **4**(5), 127 (1985).

Holmberg, A., "On the Practical Identifiability of Microbial Growth Models Incorporating Michaelis Menten Type Nonlinearities," *Math. Biosci.*, **62**, 23 (1982).

Liviense, J. C., "An Investigation of the Aerobic, Glucose-Limited Growth and Dynamics of Saccharomyces cerevisiae," PhD Thesis, Purdue University (1984).

Narendra, K. S., and A. M. Annaswamy, *Stable Adaptive System*, Prentice Hall Information and System Sciences Series, Englewood Cliffs, NJ (1989).

Nihtila, M., P. Harmo, and M. Perttula, "Real-Time Growth Estimation in Batch Fermentation," *Bridge Between Control Science and Technology, Proc. Triennial World Cong. of IFAC*, Budapest, Hungary, **4**, 1825 (1984).

Sonnleitner, B., and O. Kappeli, "Growth of Saccharomyces cerevisiae is Controlled by its Limited Respiratory Capacity: Formulation and Verification of a Hypothesis," *Biotech. Bioeng.*, **28**, 927 (1986).

Stephanopoulos, G., and K. Y. San, "Studies on On-Line Bioreactor Identification: I. Theory," *Biotech. Bioeng.*, **26**, 1176 (1984).

Manuscript received Feb. 17, 1989, and revision received Nov. 2, 1989.